CXC Receptor-2 Knockout Genotype Increases X-Linked Inhibitor of Apoptosis Protein and Protects Mice From Acetaminophen Hepatotoxicity

Bin Hu and Lisa M. Colletti

Although acetaminophen is a commonly used analgesic, it can be highly hepatotoxic. This study seeks to further investigate the mechanisms involved in acetaminophen-induced hepatotoxicity and the role of chemokine (C-X-C motif) receptor 2 (CXCR2) receptor/ligand interactions in the liver's response to and recovery from acetaminophen toxicity. The CXC chemokines and their receptor, CXCR2, are important inflammatory mediators and are involved in the control of some types of cellular proliferation. CXCR2 knockout mice exposed to a median lethal dose of acetaminophen had a significantly lower mortality rate than wild-type mice. This difference was at least partially attributable to a significantly decreased rate of apoptosis in CXCR2 knockout mice versus wild-type mice; there were no differences seen in hepatocyte proliferation in wild-type mice versus knockout mice after this injury. *Conclusion*: The decreased rate of apoptosis in the knockout mice correlated with an almost undetectable and significantly decreased level of activated caspase-3 and significantly increased levels of X-linked inhibitor of apoptosis protein, which also correlated with increased levels of nuclear factor kappa B p52 and decreased levels of c-Jun N-terminal kinase; this provides a possible mechanism for the decrease in apoptosis seen in CXCR2 knockout mice. (HEPATOLOGY 2010;52:691-702)

Acute liver failure is common in patients admitted to the intensive care unit; in approximately 20% of acute hepatic failure cases, the liver injury is related to acetaminophen (APAP) toxicity.[1] The mechanism of APAP-induced liver injury involves the cytochrome P-450–generated metabolite *N*-acetyl-*p*-benzoquinone imine, which causes glutathione (GSH) depletion, impairs mitochondrial respiration, and interferes with calcium homeostasis, although the actual events resulting in cell death are not well understood.[2]

Apoptosis occurs in all cells and is regulated by cellular death and cellular survival signals. Imbalances in these signals can be lethal and likely play a role in many pathophysiological processes. X-linked inhibitor of apoptosis protein (XIAP), which belongs to the inhibitor of apoptosis protein (IAP) family, binds to and inhibits caspase-3 and caspase-9 and protects endothelial cells against tumor necrosis factor-alpha–mediated apoptosis.[3] XIAP also inhibits apoptosis by another mechanism: a positive feedback loop that furthers nuclear factor kappa B (NF-κB) activation.[3,4]

This article investigates chemokine (C-X-C motif) receptor 2 (CXCR2) signaling in the apoptotic response to hepatic APAP toxicity in the mouse. The CXC chemokines play a role in many inflammatory and regenerative processes and are the major ligands for the CXCR2 receptor. Studies have demonstrated that CXC chemokines, including interleukin-8, macrophage inflammatory protein-2 (MIP2), and keratinocyte (KC) among others, have direct effects on hepatocytes. The CXCR2 receptor is expressed on

Abbreviations: ALT, alanine aminotransferase; APAP, acetaminophen; AST, aspartate aminotransferase; Bcl-2, B cell lymphoma 2; Bcl-XL, B cell lymphoma extra large; BrdU, bromodeoxyuridine; cIAP, cellular inhibitor of apoptosis protein; CXCR2, chemokine (C-X-C motif) receptor 2; ELISA, enzyme-linked immunosorbent assay; GAPDH, glyceraldehyde 3-phosphate dehydrogenase; GSH, glutathione; IAP, inhibitor of apoptosis protein; IB, immunoblotting; IgG, immunoglobulin G; IP, immunoprecipitation; JNK, c-Jun N-terminal kinase; KC, keratinocyte; KO, knockout; MFI, mean fluorescence intensity; MIP2, macrophage inflammatory protein-2; NF-κB, nuclear factor kappa B; PBS, phosphate-buffered saline; PCR, polymerase chain reaction; RT-PCR, reverse-transcription polymerase chain reaction; SAPK, stress-activated protein kinase; SDS-PAGE, sodium dodecyl sulfate–polyacrylamide gel electrophoresis; TUNEL, terminal deoxynucleotidyl transferase–mediated deoxyuridine triphosphate nick-end labeling; WT, wild type; XIAP, X-linked inhibitor of apoptosis protein.

From the University of Michigan, Department of Surgery, Ann Arbor, MI.

Received August 5, 2009; accepted April 6, 2010.

Address reprint requests to: Lisa M. Colletti, M.D., ?2210A Taubman, SPC 5343, 1500 East Medical Center Drive, Ann Arbor, MI 48109-0331. E-mail: colletti@umich.edu.

Published online in Wiley InterScience (www.interscience.wiley.com).

DOI 10.1002/hep.23715

Potential conflict of interest: Nothing to report.

hepatocytes,[5] and that finding has been confirmed in this study. In models of both partial hepatectomy and APAP toxicity, CXCR2/ligand interactions promote hepatocyte proliferation and liver regeneration.[4,6,7] In contrast, other investigators have found that CXCR2 ligands can be hepatotoxic.[8]

Materials and Methods

Animal Model. CXCR2-targeted mutant mice were generated by the mating of heterozygote C.129S2(B6)-Il8rb^{tm1Mwm}/J (Il8rb^{tm1Mwm}/Il8rb^{+}) mice (Jackson Laboratory, Bar Harbor, MN) in the University of Michigan animal facility. CXCR2 mutant (Il8rb^{tm1Mwm}/Il8rb^{tm1Mwm}) mice and CXCR2 wild-type (Il8rb^{+}/Il8rb^{+}) mice were used in all experiments; wild-type and mutant mice were based on the mouse 129 strain. All experiments were performed in compliance with the standards for animal use and care set by the University of Michigan's committee on the use and care of animals.

Animals were fasted overnight, and APAP or an equal volume of phosphate-buffered saline (PBS) was administered intraperitoneally.[9] For mortality experiments, animals received 750 or 1000 mg/kg APAP; for all other experiments, 375 mg/kg was used. On the basis of previous experiments with this strain of mouse, 750 mg/kg APAP is approximately the median lethal dose, and 375 mg/kg is approximately the 25% lethal dose.

To confirm that apoptosis is important in the APAP-induced liver injury in this model, additional experiments were performed with the pancaspase inhibitor Q-VD-OPh. Q-VD-OPh is more effective at preventing apoptosis than other inhibitors, such as ZVAD-fmk and Boc-D-fmk, and is nontoxic to cells, even at high doses.[10] This compound prevents apoptosis mediated by the three major apoptotic pathways: caspase-9/3, caspase-8/10, and caspase-12.[10] Q-VD-OPh (50 mg/kg; R&D Systems, Minneapolis, MN) was administered 1 hour before APAP injection; control animals received an equivalent dose of vehicle. Animals were then sacrificed according to protocol, and apoptosis was measured by terminal deoxynucleotidyl transferase–mediated deoxyuridine triphosphate nick-end labeling (TUNEL) staining and DNA fragmentation assay.

Aspartate Aminotransferase (AST) and Alanine Aminotransferase (ALT) Assay. Serum AST and ALT were measured in CXCR2 knockout and wild-type mice 24, 48, and 72 hours after APAP or PBS administration. Animals were sacrificed, their blood was collected, and the serum was separated from the clotted blood by centrifugation at 4000 rpm for 15 minutes at 4°C. ALT and AST were measured with a Diagnostics ALT and AST test kit from Sigma Chemical Co. (St. Louis, MO).

GSH Assay. Mouse livers were perfused with a perfusion medium (Gibco, Grand Island, NY) to remove intravascular blood. Ten milligrams of liver tissue was homogenized in 1 mL of PBS containing 2 mM ethylene diamine tetraacetic acid. Fifty microliters of tissue extract was used for GSH measurement. GSH was measured according to the manufacturer's instructions with a GSH assay kit (Promega, Madison, WI). Luminescence was detected with a Synergy 2 multimode microplate reader with Gen5 data analysis software (BioTek, Winooski, VT).

DNA Fragmentation Assay. DNA was extracted from 25 mg of mouse liver. Total DNA purification was performed with a DNeasy blood and tissue kit (Qiagen, Germantown, MA) according to the manufacturer's instructions. RNA was eliminated by incubation in 5 μg/mL RNase (Roche, Indianapolis, IN). A 1.5-μg DNA aliquot was loaded onto 1.5% agarose gel for separation to assess for DNA fragmentation.

TUNEL Staining. TUNEL staining was conducted with an *in situ* apoptosis detection kit from R&D Systems according to the manufacturer's instructions. Six to seven animals were used per time point per treatment group. At least 1000 cells (TUNEL-positive cells and TUNEL-negative cells) were counted in each of eight separate low-power fields for each animal, and the percentage of TUNEL-positive cells was calculated.

In Vivo *Measurement of Hepatocyte Proliferation by Bromodeoxyuridine (BrdU) Incorporation.* Two hours prior to sacrifice, animals received 30 μg of BrdU/g of body weight intraperitoneally. Liver specimens were obtained, fixed in 4% paraformaldehyde, processed for histological analysis, and stained with the Amersham cell proliferation kit (Amersham Pharmacia Biotech, Ltd., United Kingdom). BrdU incorporation was measured at 24, 36, 48, and 72 hours. There were four to seven mice per treatment group per time point. At least 1000 cells (BrdU-positive cells and BrdU-negative cells) were counted in each of eight separate low-power fields for each animal, and the percentage of BrdU-positive cells was calculated.

Cytoplasmic and Nuclear Protein Extraction. Hepatic cytoplasmic and nuclear proteins were extracted with the NE-PER nuclear and cytoplasmic extraction reagent kit (Pierce Biotechnology, Rockford, IL) according to the manufacturer's instructions.

Immunoprecipitation and Western Blot Analysis. Liver samples were homogenized in a radioimmunoprecipitation assay buffer (50 mM trishydroxymethyl-

aminomethane–hydrochloric acid, pH 7.4, 150 mM sodium chloride, 1% Nonidet P40, 0.1% sodium dodecyl sulfate, 0.25% sodium deoxycholate, 1 mM ethylene diamine tetraacetic acid, and protease and phosphatase inhibitors). Four hundred micrograms of protein was used for immunoprecipitation. The lysate was precleared with 1 μg of isotype immunoglobulin G (IgG) and 50 μL of protein A/G agarose at 4°C for 1 hour. Five micrograms of an immunoprecipitating antibody or isotype IgG was added to the supernatant, and it was rocked overnight at 4°C. Next, 50 μL of protein agarose was added, and the mixture was rocked for 2 hours at 4°C. The protein bound to the agarose conjugate was centrifuged, and the pellet was washed three times with a radioimmunoprecipitation assay buffer. Ten microliters of a 4× sodium dodecyl sulfate–polyacrylamide gel electrophoresis (SDS-PAGE) sample buffer and 5 μL of 1 M dithiothreitol were added to the pellet, and the sample was boiled for 5 minutes and centrifuged. The supernatant was saved for SDS-PAGE. Fifty micrograms of the protein lysate was subjected to SDS-PAGE under reducing conditions and transferred to polyvinylidene fluoride membranes. Blots were blocked in a 5% milk solution and exposed to anti-mouse first antibodies overnight at 4°C. First, antibodies were reacted with horseradish peroxidase–conjugated secondary antibodies. All membranes were visualized with West Pico chemiluminescent substrate (Pierce Biotechnology). Gel-Pro Analyzer software (Media Cybernetics, Bethesda, MD) was used to quantify the bands obtained via western blotting. The band optical density was normalized to the optical density of the loading control band.

Reagents for Immunoprecipitation, Western Blot Analysis, and Flow Cytometry. Antibodies for caspase-3, caspase-9, B cell lymphoma 2 (Bcl-2), B cell lymphoma extra large (Bcl-XL), phosphorylated stress-activated protein kinase (SAPK)/c-Jun N-terminal kinase (JNK; T183/Y185), and SAPK/JNK were purchased from Cell Signaling Technology, Inc. (Danvers, MA). Monoclonal anti-human/mouse cellular inhibitor of apoptosis protein 2 (cIAP2), XIAP, phycoerythrin-labeled anti-CXCR2, and phycoerythrin-labeled rat IgG2a were purchased from R&D Systems. Glyceraldehyde 3-phosphate dehydrogenase (GAPDH), NF-κB p65, NF-κB p52, anti-phosphoserine, horseradish peroxidase–conjugated goat anti-mouse IgG, and horseradish peroxidase–conjugated goat anti-rabbit IgG were purchased from Santa Cruz Biotechnology, Inc. (Santa Cruz, CA).

Hepatocyte Isolation. Primary hepatocytes were isolated by collagenase perfusion. Anesthesia was induced with isoflurane inhalation, laparotomy was performed, and the inferior vena cava was cannulated with a 26-gauge angiocatheter. A liver perfusion buffer (Gibco) was used to flush the liver of intravascular blood (3 mL/minute for 10 minutes). This was followed by the infusion of a liver digest buffer (Gibco; 3 mL/minute for 10 minutes). The liver was excised from the animal, placed in a Petri dish, minced into 1-mm pieces, and gently agitated so that the cells would be dispersed in the wash buffer (Gibco). The cell suspension was filtered and washed two times at 50*g* at 4°C for 5 minutes. Cells were immediately used for reverse-transcription polymerase chain reaction (RT-PCR) or flow cytometry.

RNA Extraction and RT-PCR. Hepatocytes were isolated as described previously. Mouse neutrophils were isolated from the pooled blood of three mice by differential gradient centrifugation over Percoll (Gibco). Total RNA from hepatocytes or neutrophils was isolated with an RNeasy mini kit (Qiagen) according to the manufacturer's instructions. The polymerase chain reaction (PCR) primers were designed with Primer Premier software (Premier Biosoft International) to cross exon 1 and exon 2. The sense primer was 5′-TGCTCACAAACAGCGTCGTA-3′. The antisense primer was 5′-TCAGGGCAAAGAACAGGTCA-3′.

Reverse transcription was performed with the QuantiTect reverse-transcription kit (Qiagen). The extracted RNA was on-column DNase-digested (RNase-free DNase set, Qiagen), and 1 μg of total RNA was reverse-transcribed into complementary DNA with the QuantiTect reverse-transcription kit (Qiagen). Real-time PCR was performed in a SYBR Green PCR master mix (Bio-Rad, Hercules, CA) with a Bio-Rad iCycler iQ multicolor real-time PCR detection system according to the following protocol: initial activation at 95°C for 15 minutes, 40 cycles at 94°C for 15 seconds, 55°C for 30 seconds, and 72°C for 30 seconds. Amplification specificity was checked by melting curve analysis and agarose gel electrophoresis.

Flow Cytometry. Hepatocytes were harvested and immediately studied with flow cytometry for CXCR2 expression. Cells were washed twice in a staining buffer (Difco, Detroit, MI), resuspended in 100 μL of the staining buffer, incubated for 15 minutes at 4°C with anti-mouse CD16/32 to block Fc receptors, and incubated for 30 minutes at 4°C with phycoerythrin-labeled anti-CXCR2 or phycoerythrin-labeled rat IgG2a. Final antibody concentrations were 1 to 2 μg/100 μL of cell solution. After incubation, cells were washed twice in the staining buffer and analyzed. Flow cytometry was performed with a FACScan cytometer (Becton Dickinson, Mountain View, CA). Data were

collected and analyzed with CellQuest software. At least 10,000 cells were analyzed to determine cell-surface CXCR2 expression.

Enzyme-Linked Immunosorbent Assay (ELISA). Fifty milligrams of mouse liver was homogenized in 1-mL of a lysis buffer containing protease inhibitors. The protein concentration was measured, and the samples were adjusted to the same protein concentrations. KC and MIP2 were measured with Quantikine murine ELISA kits (R&D Systems) according to the manufacturer's instructions. The KC and MIP2 concentrations were calculated per gram of liver protein.

Statistical Analysis. All data are expressed as means and standard errors of the mean. Statistical calculations were performed with GraphPad Prism 5 (GraphPad Software, Inc., CA) on a Macintosh PowerBook G4 computer. Statistical analysis was performed with an unpaired Student *t* test or two-way analysis of variance. Differences were considered significant if *P* was less than 0.05. Survival rates are presented with Kaplan-Meier curves, and significance was calculated with the log-rank test.

Results

CXCR2 Knockout Mice Treated with APAP Have a Lower Mortality Rate than Wild-Type Mice. Wild-type mice (n = 17) and knockout mice (n = 27) received 750 mg/kg APAP; their mortality was recorded every 24 hours for 5 days. Although CXCR2 wild-type mice had a higher mortality rate than CXCR2 knockout mice, this did not reach statistical significance (Fig. 1). Although previous experiments have suggested that 750 mg/kg APAP is the median lethal dose, neither group in this study reached this mortality rate, and this is likely why the differences did not reach statistical significance. Therefore, additional wild-type mice (n = 11) and knockout mice (n = 15) were treated with 1000 mg/kg APAP, and their mortality was measured every 24 hours for 5 days. At this increased APAP dose, the mortality rate of wild-type mice was significantly higher than that of CXCR2 knockout mice (Fig. 1A; $P < 0.01$).

Serum AST and ALT Are Lower in CXCR2 Knockout Mice Versus Wild-Type Mice After APAP. Because APAP is a hepatotoxic agent, serum AST (Fig. 1B) and ALT (Fig. 1C) were measured in knockout and wild-type mice after APAP or PBS administration. AST and ALT peaked at 24 hours, returned to the baseline at 72 hours, and were significantly lower in CXCR2 knockout mice versus wild-type mice at 24 and 48 hours. This suggests that APAP treatment in CXCR2 knockout mice caused less liver injury in comparison with wild-type mice, and this provides some explanation for the lower mortality rate in knockout mice.

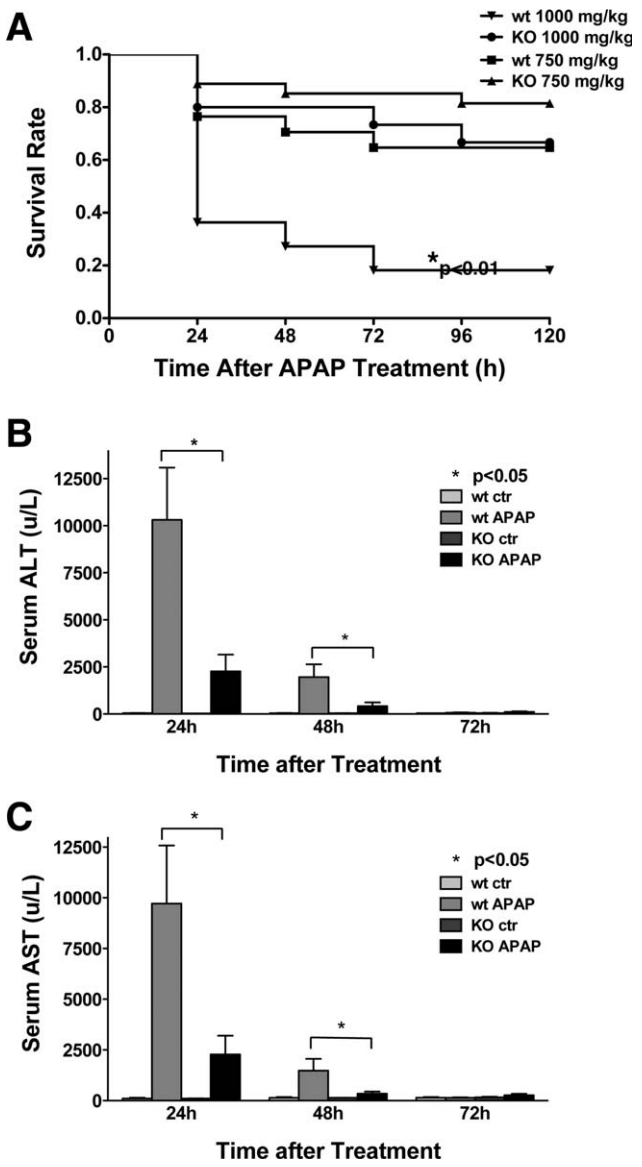

Fig. 1. (A) Mortality rate of CXCR2 knockout (KO) mice versus wild-type (WT) mice after the intraperitoneal administration of 750 or 1000 mg/kg APAP. The number of surviving animals was measured every 24 hours for 5 days. The survival curves were generated with Kaplan-Meier analysis (*$P < 0.01$ versus KO animals receiving the same APAP dose). (B) Serum ALT and (C) AST in CXCR2 KO and WT mice treated with 375 mg/kg APAP or PBS (control). Serum was collected at 24, 48, and 72 hours, and serum ALT and AST activities were determined ($n \geq 5$ per group). CXCR2 KO mice had significantly lower ALT and AST levels at 24 and 48 hours ($P < 0.05$) in comparison with WT mice.

Less Hepatocyte Apoptosis Is Seen After APAP in CXCR2 Knockout Mice Versus Wild-Type Mice. Liver injury was also investigated through the measurement

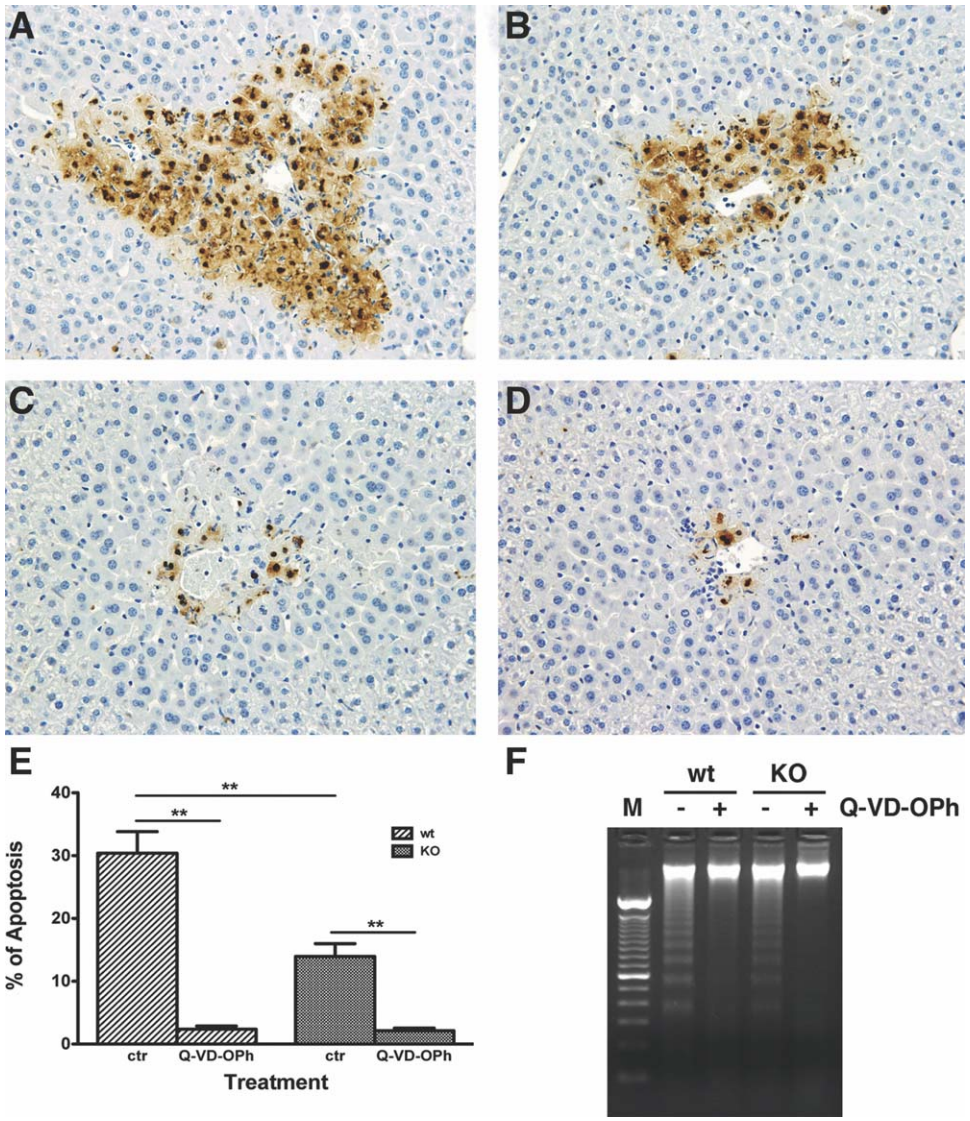

Fig. 2. (A,C) Wild-type (WT) mice and (B,D) CXCR2 knockout (KO) mice were treated with 375 mg/kg APAP (C,D) with or (A,B) without treatment with the pancaspase inhibitor Q-VD-OPh; they were sacrificed at 16 hours, and hepatocyte apoptosis was assessed by TUNEL staining (×400). (E) TUNEL-positive cells were counted, and the percentage of positive cells is illustrated (**$P < 0.01$, n = 6-9 mice per group). (F) DNA fragmentation confirmed the TUNEL staining findings (lane M presents the DNA molecular marker control). (E) The percentage of hepatocyte apoptosis in CXCR2 KO mice (n = 9, 13.95% ± 2.03%) was significantly lower than that in WT mice (n = 9, 30.39% ± 3.45%, **$P < 0.01$); these animals did not receive any pretreatment with Q-VD-OPh. This suggests that a decrease in apoptosis in CXCR2 KO mice in response to APAP toxicity may be one of the mechanisms responsible for the decrease in the mortality rate after lethal APAP dosing in CXCR2 KO mice versus WT mice. To verify that apoptosis was playing a significant role in the liver injury in this model, additional mice received the pancaspase inhibitor Q-VD-OPh (50 mg/kg) in addition to APAP. TUNEL staining demonstrated significantly less apoptosis in the livers of (C) WT mice and (D) KO mice receiving the caspase inhibitor with APAP. (E) TUNEL-positive cells were significantly decreased in the livers of both WT (2.37% ± 0.5%, n = 6) and KO mice (2.13 ± 0.41%, n = 6) receiving Q-VD-OPh and APAP in comparison with animals receiving APAP alone. (F) DNA fragmentation studies confirmed these findings.

of hepatocyte apoptosis with TUNEL staining and DNA fragmentation analysis. Less apoptosis was seen 16 hours after APAP in CXCR2 knockout mice (Fig. 2A,B) versus wild-type mice. The percentage of hepatocyte apoptosis in CXCR2 knockout mice (n = 9, 13.95% ± 2.03%) was significantly lower than that in wild-type mice (n = 9, 30.39% ± 3.45%, $P < 0.01$; Fig. 2E). Thus, less apoptosis in CXCR2 knockout mice after APAP may be a possible mechanism for the lower mortality rate after lethal APAP dosing in CXCR2 knockout mice. To verify that apoptosis was important in this liver injury, additional mice received Q-VD-OPh. TUNEL staining demonstrated significantly less hepatocyte apoptosis in both wild-type mice (2.37% ± 0.5%, n = 6) and knockout mice (2.13% ± 0.41%, n = 6; Fig. 2C-E) receiving this caspase

inhibitor and APAP. DNA fragmentation studies confirmed this finding (Fig. 2F).

There Is No Difference in Hepatocyte Proliferation Between CXCR2 Knockout and Wild-Type Mice After APAP. To determine whether differences in hepatocyte proliferation between wild-type and knockout mice might account for the differences observed in mortality, hepatocyte proliferation after APAP was measured by hepatocyte BrdU incorporation (Fig. 3A). BrdU incorporation peaked at 48 hours in both groups. Although wild-type mice had a slightly higher hepatocyte proliferation rate than knockout mice, this did not reach statistical significance.

There Is No Difference in Hepatic GSH Depletion in CXCR2 Knockout Mice Versus Wild-Type Mice After APAP. To investigate whether CXCR2 signaling affects APAP metabolism, we measured the hepatic GSH concentration in wild-type and CXCR2 knockout mice after the administration of 375 mg/kg APAP at different time points (Fig. 3B). GSH concentrations decreased within 1 hour of APAP administration and began to rebound within 24 hours. No significant differences were seen in hepatic GSH concentrations in wild-type mice versus CXCR2 knockout mice; this suggested that CXCR2 signaling does not affect APAP metabolism.

APAP Treatment Causes Hepatic Caspase-3 and Caspase-9 Activation. Apoptosis is dependent on caspase activation. Because there is less apoptosis after APAP toxicity in knockout mice versus wild-type mice, we examined hepatic caspase-3 and caspase-9 activity 1, 2, 4, and 8 hours after APAP administration. According to western blot analysis, hepatic caspase-3 and caspase-9 were activated in both wild-type and CXCR2 knockout mice within 1 hour of APAP administration (Fig. 4). Although no differences were seen in activated caspase-9 between knockout and wild-type mice (Fig. 4A,B), activated hepatic caspase-3 levels were undetectable in knockout mice, in contrast to obvious levels in wild-type mice ($P < 0.05$ at all time points; Fig. 4C,D).

XIAP Is Increased in CXCR2 Knockout Mice After APAP Administration. Because there was a difference in apoptosis after APAP dosing in CXCR2 knockout mice versus wild-type controls as well as differences in caspase-3 activation, we next investigated if there were differences in prosurvival protein expression after APAP administration. Western blotting for the antiapoptotic proteins cIAP2, XIAP, Bcl-2, and Bcl-XL was performed on hepatic tissues 1, 2, 4, and 6 or 8 hours after APAP administration. There were no differences in hepatic Bcl-2 or Bcl-XL expression (Fig. 5A-C). In contrast, cIAP2 expression increased in wild-type and CXCR2 knockout mice after APAP, with significant increases seen within 1 to 2 hours of APAP dosing; levels decreased to the baseline by 6 hours after APAP (Fig. 5D,E). Although significant cIAP increases were seen in wild-type and CXCR2 knockout mice with respect to control animals, there were no significant differences in cIAP levels in wild-type mice versus knockout mice at any time point. XIAP demonstrated the most significant differences in survival protein expression. Wild-type mice expressed minimal XIAP in response to APAP. In contrast, significant hepatic XIAP expression was seen after APAP in CXCR2 knockout mice ($P < 0.01$ at 2 and 4 hours; Fig. 5D,F).

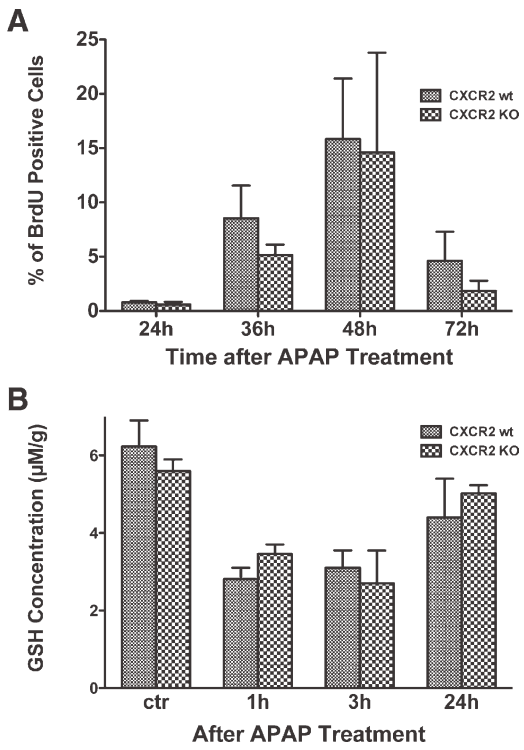

Fig. 3. (A) *In vivo* hepatocyte proliferation after APAP treatment in CXCR2 knockout (KO) and wild-type (WT) mice was measured via BrdU incorporation at various time points ($n \geq 4$ per group). Although WT mice had a slightly higher proliferation rate at all time points, none of these differences achieved statistical significance. (B) Liver GSH levels were measured after APAP treatment in WT and CXCR2 KO mice ($n = 4$-8 mice per group); no differences in GSH levels were detected between the two groups.

Hepatic NF-κB p52 Is Activated in CXCR2 Knockout Mice After APAP Administration. XIAP up-regulation is controlled by activation of NF-κB p65 and p52.[11,12] To investigate if hepatic NF-κB p65 was activated in mice after APAP administration, we measured phosphorylated NF-κB p65 by immunoprecipitation and immunoblotting at various time points after APAP dosing. There was no evidence of

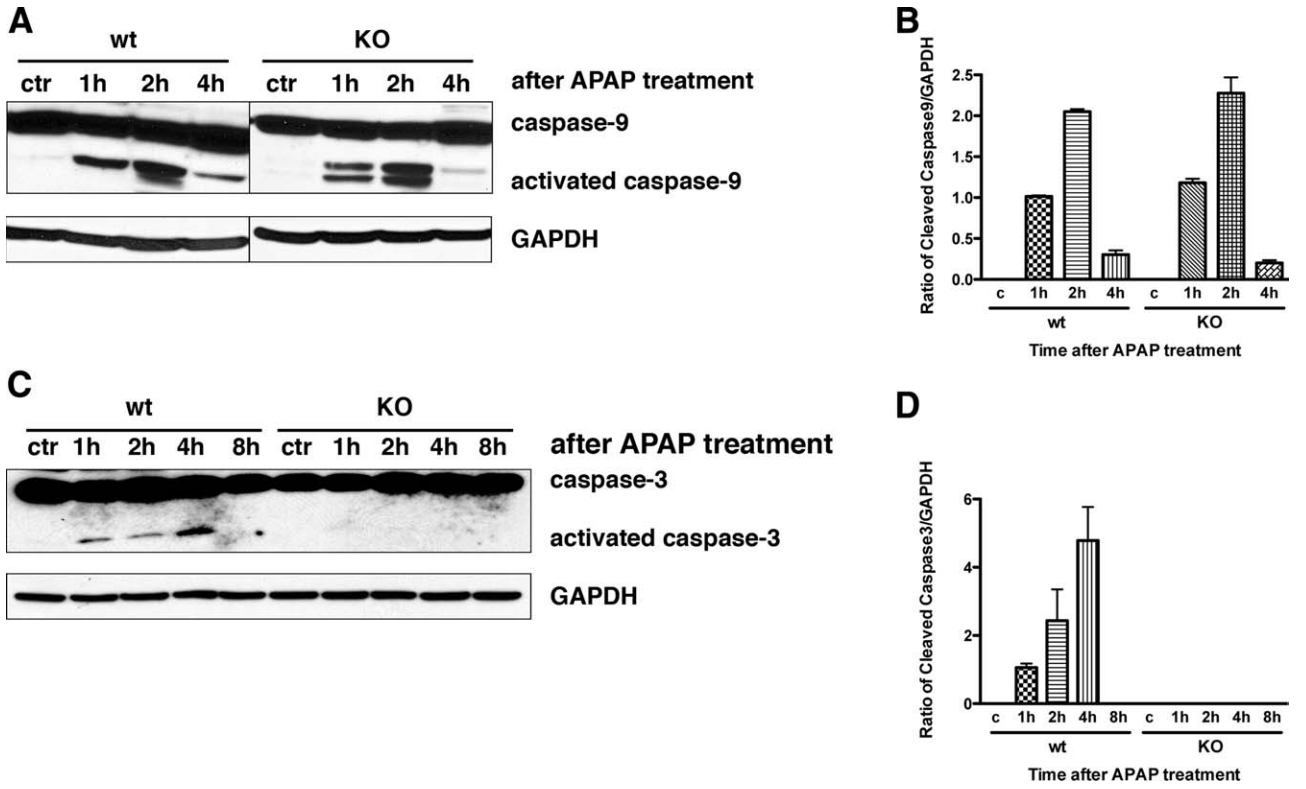

Fig. 4. Western blot analysis for activated hepatic caspase-3 and caspase-9 1, 2, 4, and 8 hours after APAP treatment in wild-type (WT) and CXCR2 knockout (KO) mice: (A,B) activated caspase-9 and (C,D) activated caspase-3. There were no differences in activated caspase-9 between WT and KO mice; in contrast, there were significant differences between levels of activated caspase-3 at all time points in WT mice versus CXCR2 KO mice ($P < 0.05$ for all time points). GAPDH levels demonstrated equal loading of the gels. Experiments were performed at least three times with similar results.

activated hepatic NF-κB p65 in wild-type or CXCR2 knockout mice after APAP (Fig. 6A). Next, we measured hepatic cytoplasmic and nuclear NF-κB p52 in knockout or wild-type mice after APAP. There was significant NF-κB p52 expression in both the cytoplasmic and nuclear hepatic proteins from CXCR2 knockout mice treated with APAP. There was no detectable hepatic NF-κB p52 after APAP in wild-type mice (Fig. 6B-D).

APAP Induces Hepatic JNK Activation in Wild-Type and CXCR2 Knockout Mice. We examined hepatic JNK expression in wild-type and CXCR2 knockout mice after the administration of 375 mg/kg APAP to investigate whether CXCR2 signaling causes JNK activation. CXCR2 knockout and wild-type mice had a significant JNK increase after APAP. Hepatic JNK activation in wild types peaked 1 hour after APAP administration, gradually declined, and returned to the baseline at 12 hours; JNK activation in CXCR2 knockout mice was slower and weaker than that in wild-type mice (Fig. 6E,F). Less JNK activation was seen in CXCR2 knockout mice versus wild-type mice; this was statistically significant at 1 hour ($P < 0.05$).

CXCR2 Expression on Mouse Hepatocytes. To determine whether the effects of CXCR2 signaling occur directly within hepatocytes rather than indirectly on other cell types within the liver, we measured CXCR2 expression on primary mouse hepatocytes; we used mouse neutrophils as a positive control because these cells are well known to express CXCR2. RT-PCR was performed with a pair of primers located in exon 2 (data not shown). These experiments confirmed CXCR2 expression on wild-type hepatocytes and neutrophils and no CXCR2 expression on CXCR2 knockout hepatocytes and neutrophils (data not shown). To exclude the possibility of contamination by genomic DNA, we designed a second pair of primers that crossed exon 1 and exon 2. These experiments confirmed that wild-type hepatocytes and neutrophils expressed CXCR2 (Fig. 7A); CXCR2 knockout hepatocytes did not express any detectable CXCR2.

Flow cytometry confirmed these results (Fig. 7B,C). Wild-type hepatocytes expressed low CXCR2 levels. There was no CXCR2 expression on knockout mouse hepatocytes. The mean fluorescence intensity (MFI) of CXCR2 on wild-type hepatocytes (5.26% $\pm$ 0.33%)

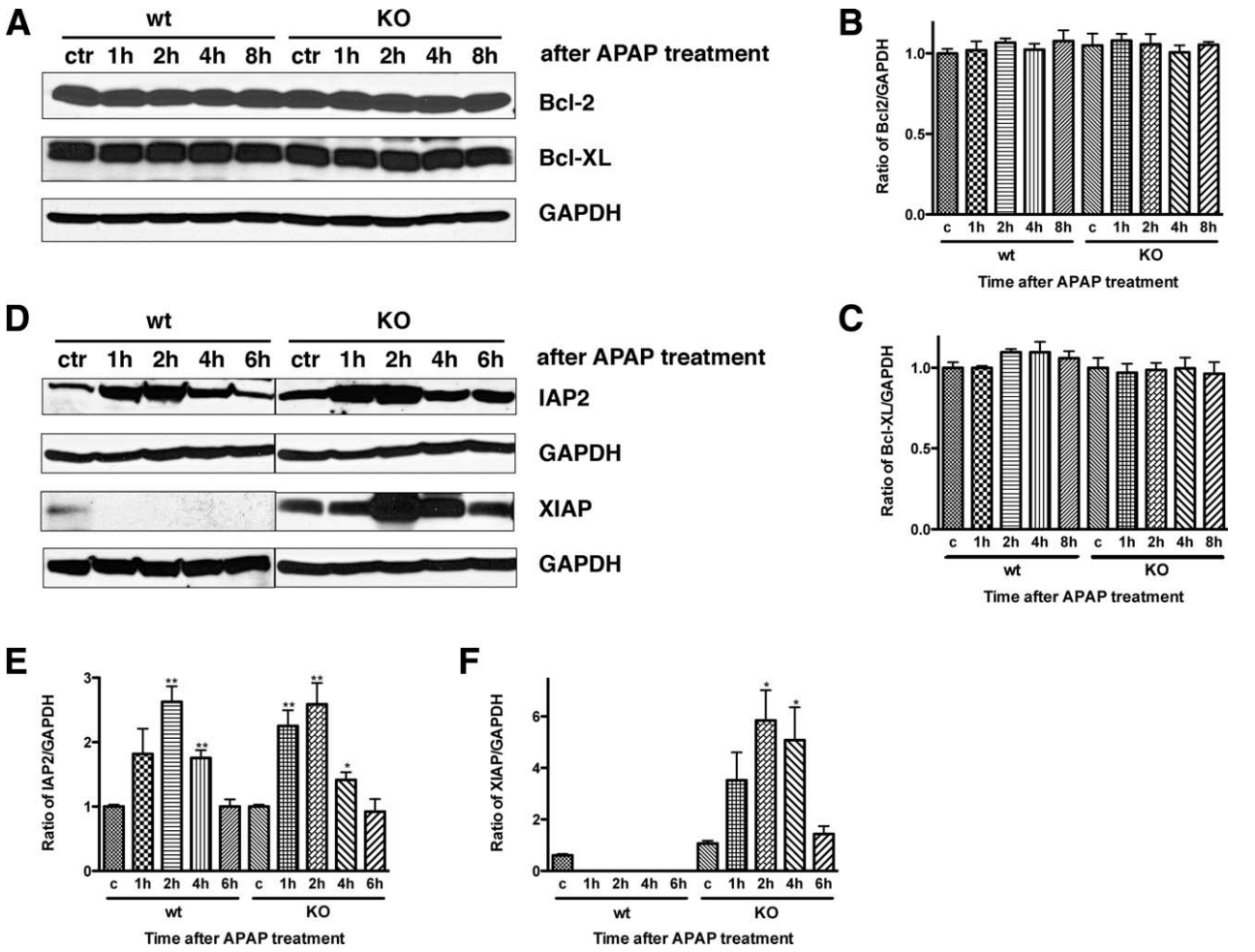

Fig. 5. Representative western blots showing hepatic expression of prosurvival proteins in CXCR2 knockout (KO) mice and wild-type (WT) controls treated with APAP. (A-C) Bcl-2 and Bcl-XL protein levels. These showed no change in response to APAP dosing in WT or CXCR2 KO mice. (D-F) Hepatic cIAP2 and XIAP protein levels. These showed differences in the response to APAP. cIAP2 levels increased in both WT and CXCR2 KO mice in response to APAP; WT levels were significantly different from those of controls at 2 and 4 hours (**$P < 0.01$), and KO levels were significantly different from those of controls at 2, 4, and 6 hours (*$P < 0.05$ and **$P < 0.01$). However, there were no significant differences between WT and KO mice at any time point. In contrast, significant increases in XIAP levels in CXCR2 KO mice were seen in response to APAP, whereas no increases in XIAP were seen in response to APAP in WT mice (**$P < 0.01$). GAPDH levels were shown to demonstrate equal loading of the gels. Experiments were performed at least three times with similar results.

was significantly increased (Fig. 7D) versus knockout mouse hepatocytes (3.42% ± 0.37%, $P < 0.05$). MFI of hepatocyte CXCR2 expression in wild-type mice 3 hours after APAP dosing was the same as that of untreated hepatocytes, and this suggested that APAP treatment does not change hepatocyte CXCR2 expression in wild-type mice (Fig. 7D).

KC and MIP2 Expression Is Increased in CXCR2 Knockout Mice After APAP Administration. Our results suggest that CXCR2 signaling facilitates apoptosis after APAP dosing. CXCR2 activation requires that CXCR2 ligands, which include KC and MIP2, bind to this receptor. We hypothesized that APAP increases KC and MIP2 production, so hepatic KC and MIP2 protein expression was measured in wild-type and knockout mice after APAP administration by ELISA (Fig. 8A,B). KC and MIP2 protein levels increased after APAP and peaked at 4 hours in both wild-type and knockout mice. KC and MIP2 levels in the CXCR2 knockout mice were significantly higher than those in the wild-type mice ($P < 0.01$) at every time point.

Discussion

These experiments show that CXCR2 knockout mice have a survival advantage over wild-type mice after a median lethal dose of APAP. The liver injury following APAP in CXCR2 knockout mice is less than that seen in wild-type mice, and this results in significantly lower levels of serum liver enzymes and less liver injury. Further experiments have suggested that this is at least partially related to less apoptosis in knockout

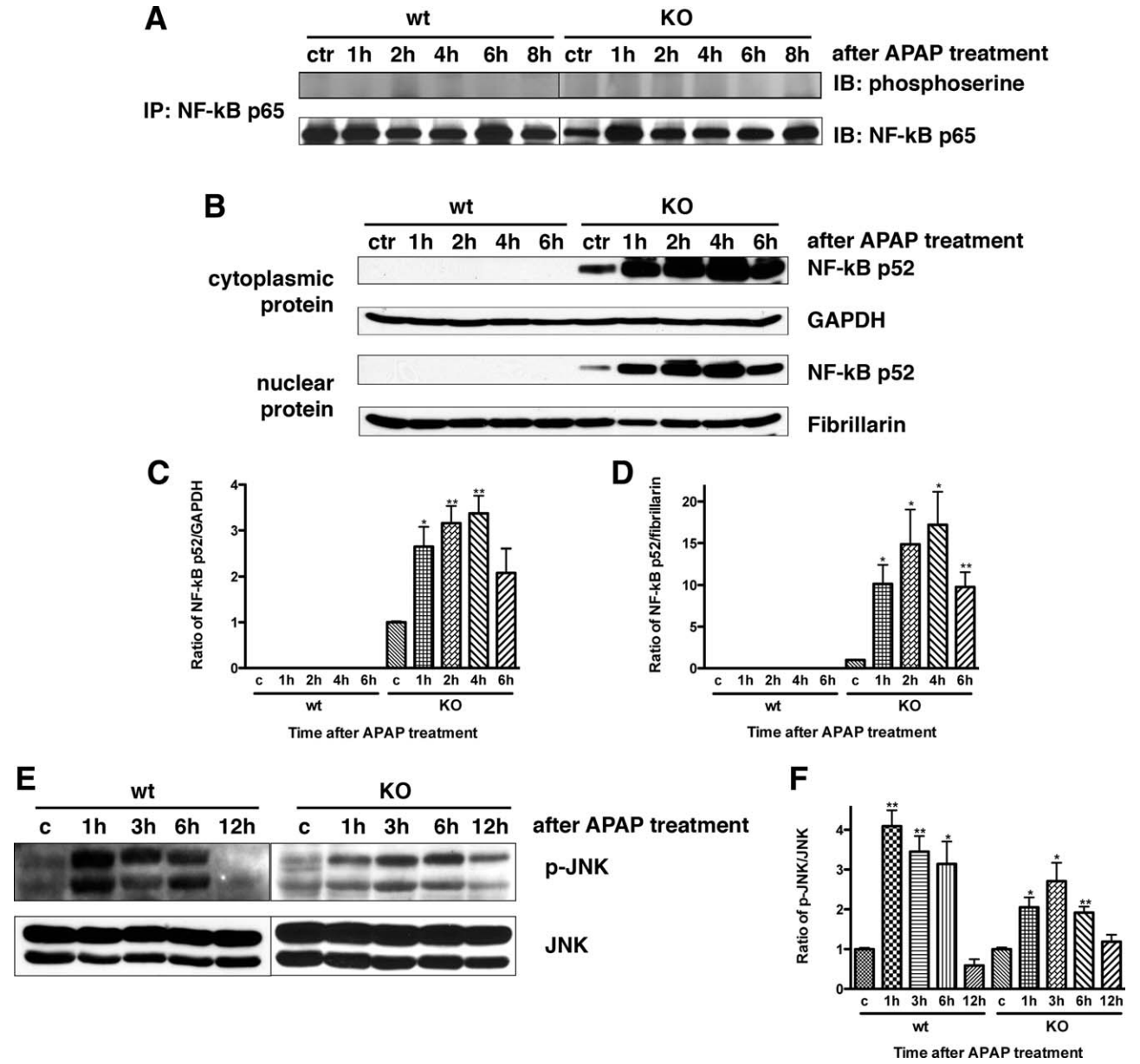

Fig. 6. (A) Activated NF-κB p65 was measured by immunoprecipitation (IP) and immunoblotting (IB) in liver tissues at various time points after APAP administration; no changes were seen in response to APAP at any time point in either wild-type (WT) or knockout (KO) mice. Next, (B,C) hepatic cytoplasmic and (B,D) nuclear proteins were extracted, and NF-κB p52 expression was examined at various time points after APAP dosing with western blotting. This demonstrated that hepatic NF-κB p52 was activated in CXCR2 KO mice in both cytoplasmic and nuclear compartments after APAP administration and was not detectable in either the cytoplasmic or nuclear proteins in WT mice after APAP (*$P < 0.05$ and **$P < 0.01$ versus WT mice at the same time point and also versus their respective controls). GAPDH was used as a cytoplasmic protein loading control, and fibrillarin was used as a nuclear protein control. (E,F) Next, activated hepatic JNK was measured by western blotting in WT and CXCR2 KO mice in response to APAP. JNK levels increased significantly in response to APAP in both CXCR2 KO mice and WT mice (*$P < 0.05$ and **$P < 0.01$ versus their respective controls). CXCR2 KO mice had less activated hepatic JNK after APAP in comparison with WT mice, and this reached statistical significance at the 1-hour time point ($P < 0.05$). Experiments were performed three times with similar results.

mice versus control animals, with no differences in hepatocyte proliferation. However, the role of apoptosis in APAP-induced liver injury is controversial, and it is possible that the less profound GSH depletion seen in this strain of mouse may allow apoptosis to proceed in a more significant fashion than that seen in other models. Although the CXCR2 receptor and its ligands, the CXC chemokines, are known to mediate the inflammatory response, these ligand/receptor interactions also modulate proliferation. For example, Bone-Larson and colleagues demonstrated increased hepatocyte proliferation after APAP injury, which was a CXCR2-dependent response.[5] This beneficial proliferative response is dependent on increased CXCR2

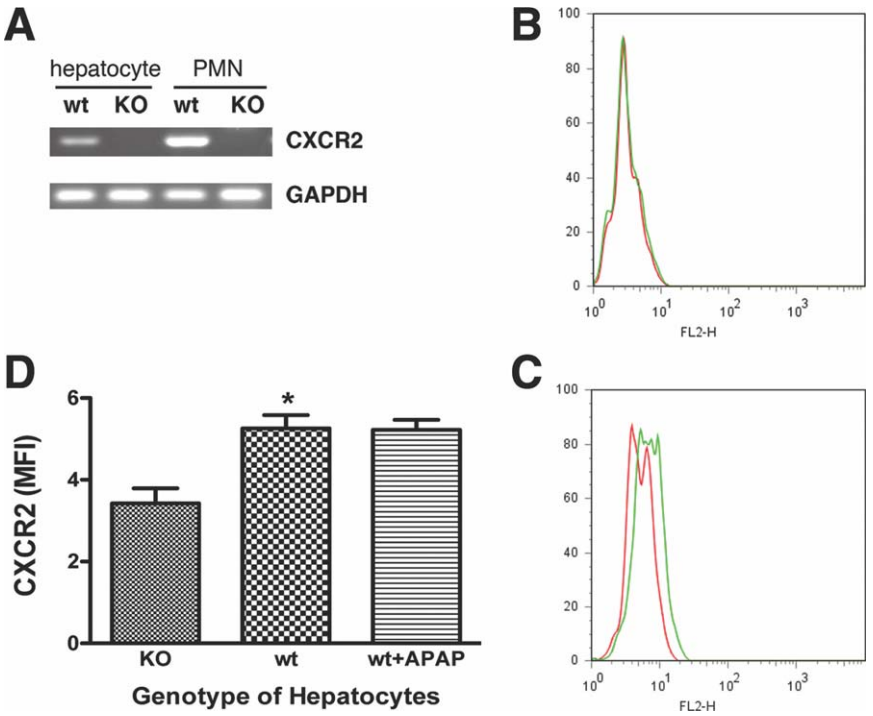

Fig. 7. (A) RT-PCR for CXCR2. Wild-type (WT) hepatocytes and neutrophils demonstrated obvious levels of CXCR2, whereas there were no detectable levels for hepatocytes or neutrophils from the CXCR2 knockout (KO) mice. GAPDH was used as a loading control. (B,C) Flow cytometry for cells expressing CXCR2. The cells were stained with phycoerythrin-conjugated isotype IgG (red line) or CXCR2 (green line). Representative histograms are shown for CXCR2 expression on (B) KO mouse hepatocytes and (C) WT mouse hepatocytes. (D) Quantitative CXCR2 expression using flow cytometry analysis by MFI ($n = 6$-12 mice per group, $*P = 0.0015$). WT mouse hepatocytes expressed low levels of CXCR2; this did not change after treatment with APAP.

expression.[5] The CXC chemokines also have a therapeutic role in APAP-induced liver injury.[5-7] This conflicts with our study, which suggests that the lack of a CXCR2 receptor/ligand interaction confers a survival benefit because of a decrease in liver injury from APAP toxicity.

Investigators have reported findings similar to ours in an ischemia/reperfusion model of injury.[13] Kuboki and others[13] demonstrated that CXCR2 knockout mice had significantly less liver injury after ischemia/reperfusion, and this was related to accelerated hepatocyte proliferation in the knockout mice. This was associated with increased NF-KB and signal transducers and activators of transcription-3 activation and was not associated with changes in inflammation.[13] These investigations suggested that low MIP2 concentrations protected against cell death, whereas high MIP2 concentrations induced cell death; these effects were absent in the CXCR2 knockout mice.[13] Similarly, Ishida and colleagues[14] also demonstrated that CXCR2 knockout mice had a lower mortality rate after APAP injury than control mice but a higher mortality rate than neutropenic mice. These findings are similar to ours in that the CXCR2 knockout genotype confers protection against hepatic injury. Our experiments did not demonstrate differences in hepatocyte proliferation, although there were significant decreases in cellular death, and the NF-κB pathway appeared to be involved in this process. Our experiments confirm the presence of the CXCR2 receptor on hepatocytes in the wild-type mice. The CXCR2 ligands, MIP2 and KC, were significantly increased after APAP in both wild-type and CXCR2 knockout mice, with the most significant increases seen in the knockout animals. The increased levels in the knockout animals did not appear to have any detrimental hepatic effects; this was similar to the results of Kuboki and colleagues.[13]

Our experiments suggest that the survival advantage conferred by the CXCR2 knockout genotype is related to decreased hepatocyte apoptosis. This was confirmed by a decrease in activated caspase-3 and increases in the prosurvival protein XIAP in CXCR2 knockout mice, and this provides a potential mechanism for decreased apoptosis. The IAP family of proteins protects against apoptosis in many systems, and this is linked to the BIF domains of these molecules, which bind to and inhibit caspases.[3] In our model, this links the decrease in activated caspase-3 to the increased XIAP levels in the knockout mice. XIAP is known to potently inhibit caspase-3, caspase-7, and caspase-9, and this also correlates with our data.[15]

Another mechanism for XIAP-conferred protection against apoptosis is a positive feedback mechanism by which XIAP induces NF-κB with the additional recruitment of other target genes.[4] XIAP as well as cIAP can activate NF-κB. cIAP is also up-regulated in our model, although this was seen in wild-type and knockout mice, so it does not provide as much of a clear explanation of the differences in these two genotypes.[4] Another interesting aspect regarding XIAP

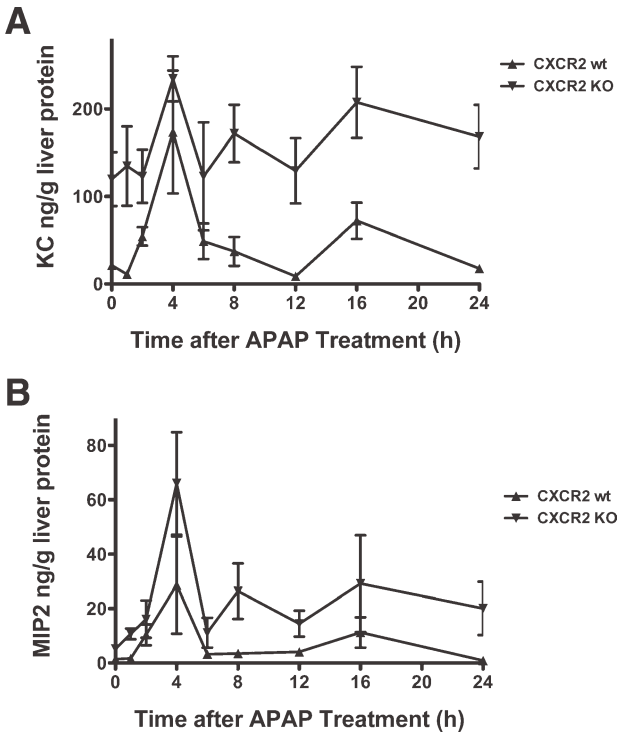

Fig. 8. APAP increased hepatic KC and MIP2 protein production in both wild-type (WT) and knockout (KO) mice (n = 4-8 mice per group per time point): (A) KC and (B) MIP2 levels. CXCR2 KO mice had significantly increased levels of each chemokine in comparison with WT controls at all time points ($P < 0.01$).

effects was demonstrated by Levkau and colleagues,[3] who showed that XIAP overexpression inhibits cell proliferation; this may suppress the cell cycle and prevent cells from exiting G0/G1 into phases of the cell cycle that are more vulnerable to apoptotic signals.

Although the classical NF-κB activation pathway is important in many cellular processes, the noncanonical NF-κB pathway is also important for normal and pathological processes. NF-κB is restricted to the cytoplasm by inhibitory proteins that are degraded when they are specifically phosphorylated; this permits NF-κB to enter the nucleus and activate target genes. Different combinations of NF-κB subunits induce transcription with different timing sequences and recognize different sequences of NF-κB binding sites. The noncanonical pathway is based on processing of the NF-κB2 gene product p100.[11,12] The p52 subunit is generated from p100 processing by I kappa B kinase alpha, one of the kinase complexes.[11,12] Once produced, p52 can enter the nucleus and induce genes that regulate many processes.[12] In other systems, including androgen-sensitive LNCaP cells *in vitro* and lymphoma cells, NF-κB/p52 encourages cellular growth by protecting cells from apoptosis and stimulating cyclin D1 expression.[16,17] Coculturing of bone marrow stromal cells with lymphoma cells resulted in active p52 generation, which then translocated to the nucleus and was associated with increased XIAP and cIAP expression; this was similar to what was seen in our system.[17]

Investigators have shown a significant relationship between NF-KB, XIAP, and the JNK cascade.[18-20] Bubici and colleagues[18] showed that NF-KB–mediated apoptosis suppression involves inhibition of the JNK cascade, which is related to up-regulation of a variety of mediators, including XIAP, which block aspects of the JNK cascade. Similarly, Kaur and colleagues[20] showed that XIAP inhibits JNK activation by transforming growth factor β1 and counteracts transforming growth factor β1–induced apoptosis. This is consistent with our findings, in which CXCR2 knockout mice increased XIAP levels, decreased JNK levels, and decreased apoptosis and mortality. Other investigators have used leflunomide with APAP toxicity and have shown a protective effect due to the inhibition of APAP-induced JNK activation. This decreased Bcl-2 and Bcl-XL activation and decreased apoptosis.[19] This is also consistent with our studies. In contrast, other investigators have shown that APAP-induced activation of JNK promotes necrosis by a direct effect on mitochondria.[21,22]

References

1. Sakil AO, Kramer D, Mazariegos GV, Fung JJ, Rakela J. Acute liver failure: clinical features, outcome analysis and applicability of prognostic criteria. Liver Transpl 2000;6:163-169.
2. Dahlin DC, Miwa GT, Lu AY, Nelson SD. *N*-Acetyl-*p*-benzoquinone imine: a cytochrome P-450-mediated oxidation product of acetaminophen. Proc Natl Acad Sci U S A 1984;81:1327-1331.
3. Levkau B, Garton KJ, Ferri N, Kloke K, Nofer JR, Baba HA, et al. xIAP induces cell-cycle arrest and activates nuclear factor-κB. New survival pathways disabled by caspase-mediated cleavage during apoptosis of human endothelial cells. Circ Res 2001;88:282-290.
4. Chu ZL, McKinsey TA, Liu L, Gentry JJ, Malim MH, Ballard DW. Suppression of tumor necrosis factor-induced cell death by inhibitor or apoptosis, c-IAP is under NF-KB control. Proc Nat Acad Sci U S A 1997;94:10057-10062.
5. Bone-Larson CL, Hogaboam CM, Evanhoff H, Strieter RM, Kunkel SL. IFN-gamma-inducible protein-10 (CXCL10) is hepatoprotective during acute liver injury though induction of CXCR2 on hepatocytes. J Immunol 2001;167:7077-7083.
6. Hogaboam CM, Bone-Larson CL, Steinhauser ML, Lukas NW, Colletti LM, Simpson KJ, et al. Novel CXCR2-dependent liver regenerative qualities of ELR containing CXC chemokines. FASEB J 1999;13:1565-1574.
7. Ren X, Carpenter A, Hogaboam C, Colletti L. Mitogenic properties of endogenous and pharmacologic doses of macrophage inflammatory protein-2 after 70% hepatectomy in the mouse. Am J Pathol 2003;163:563-570.
8. Stefanovic L, Brenner DA, Stefanovic B. Direct hepatotoxic effect of KC chemokine in the liver without infiltration of neutrophils. Exp Biol Med 2005;230:573-586.

9. Kofman AV, Morgan G, Kirschenbaum A, Osbeck J, Hussain M, Swenson S, et al. Dose- and time-dependent oval cell reaction in acetaminophen-induced murine liver injury. HEPATOLOGY 2005;41:1252-1261.
10. Caserta TM, Smith AN, Gultice AD, Reedy MA, Brown TL. Q-VD-OPh, a broad spectrum caspase inhibitor with potent antiapoptotic properties. Apoptosis 2003;8:345-352.
11. Wietek C, Cleaver CS, Ludbrook V, Wilde J, White J, Bell DJ, et al. IkappaB kinase epsilon interacts with p52 and promotes transactivation via p65. J Biol Chem 2006;281:34973-34981.
12. Xiao G, Rabson AB, Young W, Qing G, Qu Z. Alternative pathways of NF-kappaB activation: a double-edged sword in health and disease. Cytokine Growth Factor Rev 2006;17:281-293.
13. Kuboki S, Shin T, Huber N, Eismann T, Galloway E, Schuster R, et al. Hepatocyte signaling through CXC chemokine receptor-2 is detrimental to liver recovery after ischemia/reperfusion in mice. HEPATOLOGY 2008;48:1213-1223.
14. Ishida Y, Kondo T, Kimura A, Tsuneyama K, Takayasu T, Mukaida N. Opposite roles of neutrophils and macrophages in the pathogenesis of acetaminophen-induced acute liver injury. Eur J Immunol 2006;36:1028-1038.
15. Deverauz QL, Roy N, Stennicke HR, Van Arsdale T, Zhou Q, Srinivasula SM, et al. IAPs block apoptotic events induced by caspase-8 and cytochrome c by direct inhibition of distinct caspases. EMBO J 1998;17:2215-2223.
16. Nadiminty N, Chun JY, Lou W, Lin X, Gao AC. NF-kappaB2/p52 enhances androgen-independent growth of human LNCaP cells via protection from apoptotic cell death and cell cycle arrest induced by androgen-deprivation. Prostate 2008;68:1725-1733.
17. Lwin T, Hazlehurst LA, Li Z, Dessureault S, Sotomayor E, Moscinski LC, et al. Bone marrow stromal cells prevent apoptosis of lymphoma cells by upregulation of anti-apoptotic proteins associated with activation of NF-kappaB(RelB/p52) in non-Hodgkin's lymphoma cells. Leukemia 2007;21:1521-1531.
18. Bubici C, Papa S, Pham CG, Zazzeroni F, Franzoso G. NF-KB and JNK. An intricate affair. Cell Cycle 2004;3:1524-1529.
19. Latchoumycandane C, Goh CW, Ong MMK, Boelsterli UA. Mitochondrial protection by the JNK inhibitor leflunomide rescues mice from acetaminophen-induced liver injury. HEPATOLOGY 2007;45:412-421.
20. Kaur S, Wang F, Venkatraman M, Arsura M. X-linked inhibitor of apoptosis (XIAP) inhibits c-jun-N-terminal kinase 1 (JNK1) activation by transforming growth factor β1 (TGF-β1) through ubiquitin-mediated proteosomal degradation of the TGF-β1-activated kinase 1 (TAK1). J Biol Chem 2005;280:38599-38608.
21. Gunawan BK, Liu ZX, Han D, Hanawa N, Gaarde WA, Kaplowitz N. c-Jun N-terminal kinase plays a major role in murine acetaminophen hepatotoxicity. Gastroenterology 2006;131:165-178.
22. Hanawa H, Shinohara M, Saberi B, Gaarde WA, Han D, Kaplowitz H. Role of JNK translocation to mitochondria leading to inhibition of mitochondrial bioenergetics in acetaminophen-induced liver injury. J Biol Chem 2008;283:13565-13577.